Advanced Robotics, Vol. 2, No. 3, pp. 241–257 (1987)
© 1988 VSP and
Robotics Society of Japan.

Paper

Force detection and active power assistance of a direct-drive manipulator

HIROHIKO ARAI and SUSUMU TACHI
Mechanical Engineering Laboratory, MITI, 1–2, Namiki, Tsukuba Science City, Ibaraki-ken, 305 Japan

Received for *JRSJ* 21 May 1985; English version received 13 November 1986

Abstract—When a manipulator is handled manually, it is necessary to reduce the reaction force caused by inertia, friction, gravity, etc. This paper describes an active power assistance system for a direct-drive manipulator, which assists the handling force with a motor, and a force detection system for that purpose. This method detects the handling force by a combination of motor torque detection with a motor current and rotation detection with internal sensors (tacho-generator, etc.). It does not need special force sensors. Some configurations of the power assistance system are also shown. The effectiveness of the proposed method is demonstrated by feasibility experiments.

1. INTRODUCTION

As one of the operational modes of a manipulator, the operator often has to apply force directly to the manipulator by his hand to move it. In the 'direct teaching' of an industrial robot involved in painting or welding, the operator programs the robot by holding the tip of the arm and moving it. In a master–slave manipulator system, the operator moves the master arm manually to control the slave arm in the work site.

In the manipulator usage mentioned above, the manipulator requires a large manual force due to the inertia of the arm, friction, gravity, etc., and this prevents quick and dextrous manipulation. Therefore it is necessary to assist the power of the operator so that he is able to move the arm easily with a small force. Passive power assistance has been employed in some commercially available industrial robots; in these cases the gravitational force is compensated by balance weights or springs while the motors are separated by electromagnetic clutches. This method, however, does not reduce the inertia or the friction. Moreover, employing balance weights results in an increase of the inertia. In some master–slave manipulators, gravity is compensated by motors. Nevertheless, neither inertia nor friction is compensated.

Another method is available in which active power assistance with actuators is implemented based on the manual force detected by a force sensor at the tip of the arm [1]. Using a sensor to detect the manual force is a direct and simple method, but it does lead to some problems:

(1) Strain gauges whose signals are weak and sensitive to the environment are now generally used in a force sensor. Therefore, stability and reliability are not sufficient.
(2) To detect the force in various directions, the sensor must inevitably have a complex structure, and conversion calculations are required to separate the signal in each direction.
(3) In addition to the conventional internal joint sensor system, such as rotary

encoders, tacho-generators, etc., an external force sensor system is necessary. This leads directly to an increase in cost.

(4) The force sensor mounted at the end of the arm detects the local force and cannot detect interference or collision in the intermediate part of the arm.

For the reasons mentioned above, the use of a force sensor does not seem to be a suitable method for active power assistance, which does not need as sensitive a force detection as that required in assembly tasks.

If it were possible to detect the manual force using only internal joint sensors such as encoders and tacho-generators, which are necessarily provided in a conventional manipulator, it would be very useful. Inoue [2] and Kurono [3] have presented methods of detecting the external force and the controlling force, both using internal joint sensors only. In addition, Uchiyama [4] has reported a method using dynamic compensation. Uchiyama's method can be applied theoretically to power assistance because of its dynamic compensation. However, it was assumed that the external force acts in a direction opposite to the motor torque resisting the servo stiffness and power assistance was not considered. In addition, a manipulator with gear reduction was employed in the experimental equipment. Therefore, the detection was not sufficient for use in power assistance.

In order to meet the recent requirement for a faster and more precise manipulator, a number of studies have been carried out concerning direct-drive manipulators which do not have any transmission mechanism between the motor and the joint [5, 6]. Applications of such manipulators to industrial robots have also been presented [7]. Direct-drive manipulators will be common in the future. In this paper, we present a method of providing active power assistance with only internal joint sensors in a direct-drive manipulator. We also demonstrate the effectiveness of power assistance experimentally. The method directly detects the joint torque with a motor current, to which the dynamic torque compensation with the signal of the internal sensor is added to detect the external force. With the direct-drive system, the external force in the same direction as that of the motor torque can be detected accurately enough for power assistance. The torque is controlled directly by the motor current based on the detected manual force, thus allowing a simple and quick response active power assistance system.

2. DETECTION OF THE MANUAL FORCE

2.1. Comparison between manipulators with gear reduction and direct-drive manipulators

Before studying manual force detection, we will compare a conventional manipulator employing reduction gears with a direct-drive manipulator. In order to extract the manual force from the internal sensors' information only, it is necessary to calculate the compensation based on a dynamic model of the arm.

In a manipulator with gear reduction, a motor rotor is connected to an arm link through the backlash and elasticity contained in the reduction gears. As a result, the displacement of the rotor is not equal to that of the link. Moreover, the inertia of the rotor and the friction generated in the reduction gears and the motor brush is not negligible compared with the inertia and friction of the link itself. Therefore, the motor torque is not equal to the drive torque applied to the link.

Even if such a complex model is employed, it is possible to obtain the manual force from the model theoretically. However, a time lag arises from the backlash and elasticity in this case. Furthermore, the unknown parameters (backlash, friction, etc.) included in the model vary significantly, and the value of the manual force to be detected may be buried in the change of these parameters.

In a direct-drive system, a motor rotor is connected directly to an arm link so that the displacement of the rotor directly represents the displacement of the link and a whole motor torque is applied to the arm. Friction may be treated as the sum of the motor friction and the link friction. Thus the model is greatly simplified. In addition, it is free from the significant friction generated in reduction gears. Since the friction itself is small, a change of the parameters hardly affects the force detection.

From the above comparison it may be gathered that a direct-drive system is expected to realize manual force detection and power assistance without using a force sensor far more easily than a gear reduction system.

2.2. Method of detecting the manual force

Manual force detection is fundamentally based on the principles given below. First, the motion of the manipulator is measured with internal sensors, e.g. encoders and tachogenerators, and the joint torque which causes the motion is estimated. Next, the drive torque with the motor is estimated from the motor current. The difference between them is considered to be the torque caused by the manual force.

First, a single-link direct-drive manipulator is considered. The relation between the torque acting on a joint and its motion can be written as

$$T_m(I)+T_o=J\ddot{\theta}+F_b\dot{\theta}+F_c+g(\theta) \tag{1}$$

where θ is the motor angle, I is the motor current, $T_m(I)$ is the motor torque, T_o is the torque caused by the manual force, J is the sum of the motor and the arm inertia moments, F_b is the viscous friction coefficient, F_c is the Coulomb friction, and $g(\theta)$ is the torque due to a potential, such as gravity.

In the case of a DC motor, when its torque constant is K_t, the motor torque $T_m(I)$ may be expressed as

$$T_m(I)=K_tI. \tag{2}$$

The Coulomb friction F_c may be separated into static and dynamic Coulomb friction. Static Coulomb friction represents the frictional torque when the motor is stationary or $\dot{\theta}=0$. It is defined as the maximum value and it balances the sum of the torque acting on the joint below that value. Dynamic Coulomb friction, which represents the frictional torque at $\dot{\theta}\neq 0$, is constant, and its sign depends on the motor rotation. It may be expressed as

$$\begin{cases} F_c = F_{dyn} & (\dot{\theta}>0) \\ F_c = -F_{dyn} & (\dot{\theta}<0) \end{cases} \tag{3}$$

(where F_{dyn} is a constant). The system described above is shown in Fig. 1.

We can obtain the following relation from equation (1):

$$T_o=J\ddot{\theta}+F_b\dot{\theta}+F_c+g(\theta)-T_m(I). \tag{4}$$

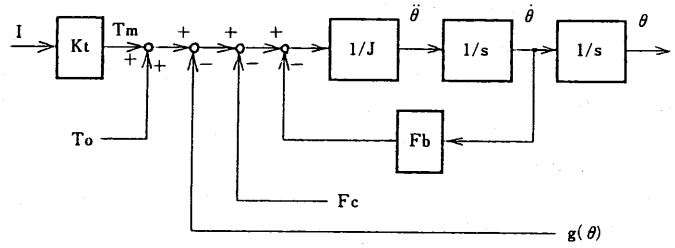

Figure 1. Block diagram of the control system.

All the terms on the right-hand side of equation (4), except F_c with $\dot{\theta}=0$ (static Coulomb friction), are functions of θ, $\dot{\theta}$, $\ddot{\theta}$, and I. θ, $\dot{\theta}$, $\ddot{\theta}$, and I can actually be measured. The parameters contained in these functions can be identified through measurements or from design specifications.

The detected manual force T_o will be given by

$$\hat{T}_o=\hat{J}\ddot{\theta}+\hat{F}_b\dot{\theta}+\hat{F}_c+\hat{g}(\theta)-\hat{T}_m(I) \tag{5}$$

while the parameters or functions so obtained are marked with a circumflex. A block diagram of the detection system is shown in Fig. 2.

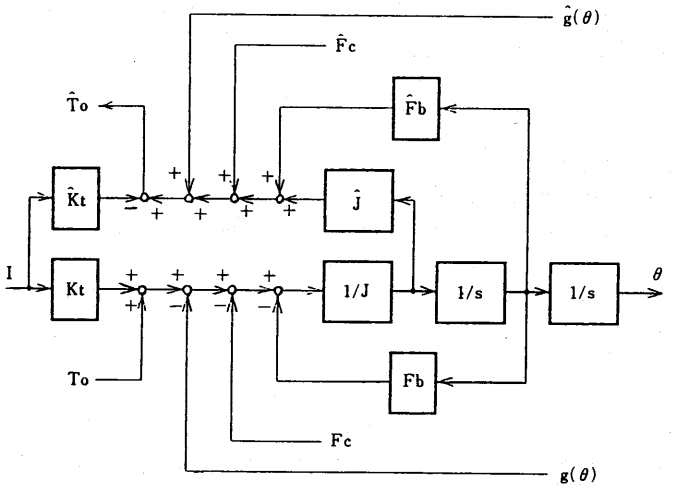

Figure 2. Block diagram of the torque detection system.

In a multiple-link manipulator, the inertia torque is affected by several links, and a coupled torque, such as the Coriolis force and centrifugal force arises. For the ith joint, the detected manual torque $\hat{T}_{oi}$ may be obtained from

$$\hat{T}_{oi}=\sum_{j=1}^{n}\hat{J}_{ij}(\boldsymbol{\theta})\ddot{\theta}_j+\sum_{j=1}^{n}\sum_{k=1}^{n}\hat{D}_{ijk}(\boldsymbol{\theta})\dot{\theta}_j\dot{\theta}_k+\hat{F}_{bi}\dot{\theta}_i$$
$$+\hat{F}_{ci}+\hat{g}_i(\boldsymbol{\theta})-\hat{T}_{mi}(I_i) \tag{6}$$

where $\theta = (\theta_1, \ldots, \theta_n)$, θ_i is the angle of the ith joint, I_i is the motor current on the ith joint, $J_{ij}(\theta)$ is the effective inertia moment of the ith joint on the jth joint, $D_{ijk}(\theta)$ is the coupled torque coefficient of the jth and kth joints on the ith joint, $g_i(\theta)$ is the potential torque such as gravity, F_{ci} is the Coulomb friction on the ith joint, and $T_{mi}(I_i)$ is the motor torque on the ith joint.

The first term, inertia, the second term, the coupled torque, and the fifth term, gravity, can be calculated from motion equations representing the dynamic characteristic of the arm.

2.3. Comparison with the force sensor system

The proposed method of manual force detection is compared with the conventional method using a force sensor.

In equation (6), the manual force is represented in the form of a torque applied to a joint. Active power assistance does not require the value of the manual force itself applied to the tip of a manipulator. Once the torque produced by manual force is obtained, it can be used directly for control. As gathered from equation (6), the amount of calculation required is on the same level of feedforward dynamic torque compensation as in ordinary position control. In this method, calculations are essential for detection. Even when a force sensor is employed, calculations are still required. Even if a simple force feedback system is used for active power assistance, calculations will be required at least for the conversion from sensor coordinates to joint coordinates. If the dynamic compensation is also to be covered, the force sensor method will require more calculations than the method proposed here.

The first four terms on the right-hand side of equation (6) have the same form as the feedforward compensation term in ordinary position control. In the recent manipulator aimed at higher speed and higher precision, the feedforward compensation is often used together [6]. In a manipulator in which an algorithm or a special processor is implemented for that calculation, actually measured values instead of desired values for positioning might be easily applied to the manual force detection. Thus, the controller does not require much supplementary hardware or software.

Moreover, in the proposed method the manual force is detected at each joint. It is possible, therefore, to detect a collision in the middle of the arm and the difference between the parameters contained in equation (6) and the real ones. Once these are detected as the manual force, the torque is controlled accordingly in active power assistance. Thus, it has the feature that no excessive force is applied on the manipulator. This cannot be detected by a force sensor at the tip of the arm.

2.4. Detection requirements and feasibility

Below, we show that each value on the right-hand side of equation (6) can be obtained through calculations or measurements. The following three requirements must be satisfied in order for the manual force to be detected from equation (6):

(1) The form of functions such as $\hat{J}_{ij}(\theta)$, $\hat{D}_{ijk}(\theta)$, and $\hat{g}_i(\theta)$ to calculate each torque term can express the actual torque correctly.
(2) The parameters contained in functions can be correctly identified.
(3) Variables θ, $\dot{\theta}$, $\ddot{\theta}$, and I_i can be measured correctly in real time.

First of all, (1) and (2) above will have to be considered carefully. It is possible to determine correctly the form of the functions for the first inertia term, the second coupled torque term, and the fifth potential torque term on the right-hand side of equation (6) based on the dynamics of the manipulator and the physical arrangement of the arm. The parameters can be calculated correctly based on the link dimensions, mass distribution, etc. Whether or not the motor torque in the sixth term is generated under equation (2) depends on the performance of the motor. Generally, motors used in a direct-drive manipulator have excellent linearity and a low torque ripple of less than several per cent. The third and fourth friction terms are mainly caused by the friction of brushes in the motor and tacho-generator. These friction terms may be considered the most difficult to obtain and the most unstable in equation (6). However, one of the features of a direct-drive manipulator is its low friction. Therefore, friction scarcely affects the manual force detection. Generally, the friction caused by the brushes consumes approximately 7–8% of the motor rated torque. It is likely that the influence of friction will be reduced further if brushless motors and rotary sensors are used in the future [8].

Next, we will discuss the measurement accuracy of the variables referred to in (3). The angle θ is measured accurately with rotary encoders. The angular velocity $\dot{\theta}$ and angular acceleration $\ddot{\theta}$ are measured by tacho-generators. Because of the slow rotation, $\dot{\theta}$ and $\ddot{\theta}$ are under the influence of ripples. However, a variety of highly accurate angle detection devices have been developed for direct-drive manipulators [9]. Using these devices will reduce the influence of ripples. Although the motor current can be easily detected, it is necessary to cut high frequency when the current is controlled in a PWM method. A current control servo amplifier with internal current feedback has a quick response and a high linearity so that the output current value may be considered to be proportional to the input voltage. In this case, use of the input voltage instead of the motor current will eliminate the influence of high-frequency noise due to switching in the PWM control.

3. ASSISTING MANUAL FORCE

3.1. Constant gain system

Active power assistance is performed based on the detected manual torque by the method referred to in Section 2. First, the active power assistance of a single-link manipulator is considered. The term, active power assistance signifies that the motor torque $T_m(I)$ is controlled so that the torque T_o caused by the manual force will be most effective in the relation given by equation (1). Using the detected manual torque $\hat{T}_o$ obtained from equation (5), assume that

$$T_m(I)=(G-1)\hat{T}_o+\hat{g}(\theta). \tag{7}$$

Then we can obtain

$$(G-1)\hat{T}_o+T_o=J\ddot{\theta}+F_b\dot{\theta}+F_c+g(\theta)-\hat{g}(\theta). \tag{8}$$

If $\hat{T}_o \fallingdotseq T_o$ and $\hat{g}(\theta)\fallingdotseq g(\theta)$, we can obtain

$$GT_o \fallingdotseq J\ddot{\theta}+F_b\dot{\theta}+F_c. \tag{9}$$

From equation (9), it may be gathered that an effect has appeared as if the manual force were multiplied by G while the gravitational torque reached zero.

$$T_m(I) = K_t K_a V_{in} \tag{10}$$

where K_t is the motor torque constant, K_a is the servo amplifier voltage–current amplification rate, and V_{in} is the servo amplifier input voltage. Then if the input voltage is

$$V_{in} = \{(G-1)\hat{T}_o + \hat{g}(\theta)\}/(\hat{K}_t \hat{K}_a) \tag{11}$$

we can obtain the motor driving torque as shown in equation (7). Figure 3 shows the block diagram.

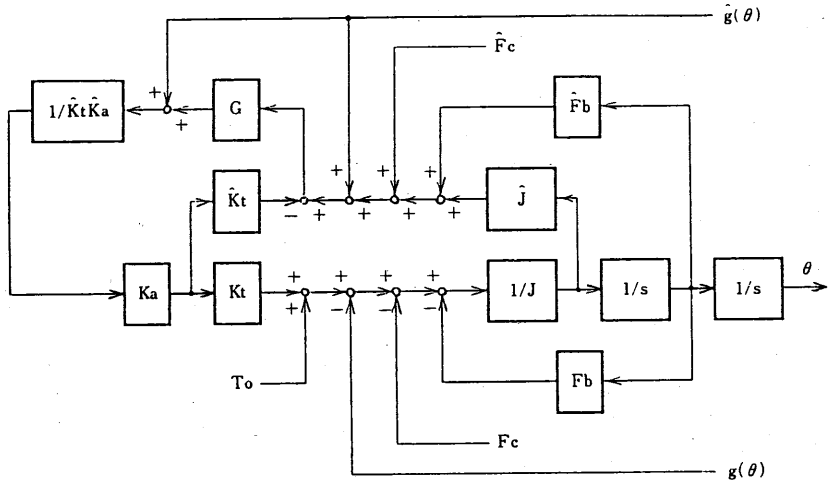

Figure 3. Block diagram of the active power assistance system (1).

If the value of the manual force is not required, the system shown in Fig. 3 can be simplified. Assume that

$$\hat{T}_m(I) = \hat{K}_t \hat{K}_a V_{in} \tag{12}$$

and eliminate T_o from equations (5), (11), and (12). Then we can get

$$V_{in} = \left\{\left(1 - \frac{1}{G}\right)(\hat{J}\ddot{\theta} + \hat{F}_b\dot{\theta} + \hat{F}_c) + \hat{g}(\theta)\right\} \Big/ (\hat{K}_t \hat{K}_a). \tag{13}$$

Figure 4 shows a block diagram which substantially allows dispensing with the detection of a current. Thus power assistance will be available using internal sensors only.

In a multiple-link manipulator, an expression equivalent to equation (7) may be obtained as follows, using $\hat{T}_{oi}$ obtained from equation (6):

$$T_{mi}(I_i) = (G_i - 1)\hat{T}_{oi} + \hat{g}_i(\theta). \tag{14}$$

If the motor torque on the ith joint is given as in the above expression, an effect will appear as if the manual force applied to the ith joint were multiplied by G_i.

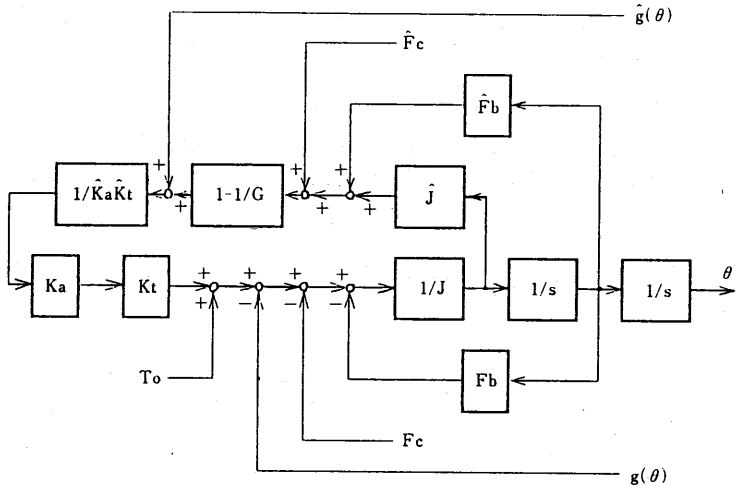

Figure 4. Block diagram of the active power assistance system (2).

3.2. *Variable parameter system*

If V_{in} is eliminated from equations (1), (10), and (13), we can obtain

$$T_o=\left\{J-\left(1-\frac{1}{G}\right)\frac{K_tK_a}{\hat{K}_t\hat{K}_a}\hat{J}\right\}\ddot{\theta}$$

$$+\left\{F_b-\left(1-\frac{1}{G}\right)\frac{K_tK_a}{\hat{K}_t\hat{K}_a}\hat{F}_b\right\}\dot{\theta}$$

$$+\left\{F_c-\left(1-\frac{1}{G}\right)\frac{K_tK_a}{\hat{K}_t\hat{K}_a}\hat{F}_c\right\}$$

$$+(g(\theta)-\underline{\hat{g}(\theta)}). \tag{15}$$

The underlined portions represent the result of power assistance. The method referred to above therefore implies that the manipulator inertia and friction coefficient have apparently decreased. In the case of Section 3.1, the decrease rate involved is generally dependent on the value of G. However, each decrease rate is now considered independent. In other words, assume that

$$T_m(I)=\alpha\hat{J}\ddot{\theta}+\beta\hat{F}_b\dot{\theta}+\gamma\hat{F}_c+\delta\hat{g}(\theta) \tag{16}$$

and we can obtain

$$T_o=(J-\alpha\hat{J})\ddot{\theta}+(F_b-\beta\hat{F}_b)\dot{\theta}+F_c-\gamma\hat{F}_c+g(\theta)-\delta\hat{g}(\theta). \tag{17}$$

Figure 5 shows the block diagram. With the manipulator inertia and friction changed independently, handling feeling is selectable. When a weak potential force is applied, it is possible to let the arm return automatically to the 'home' position when

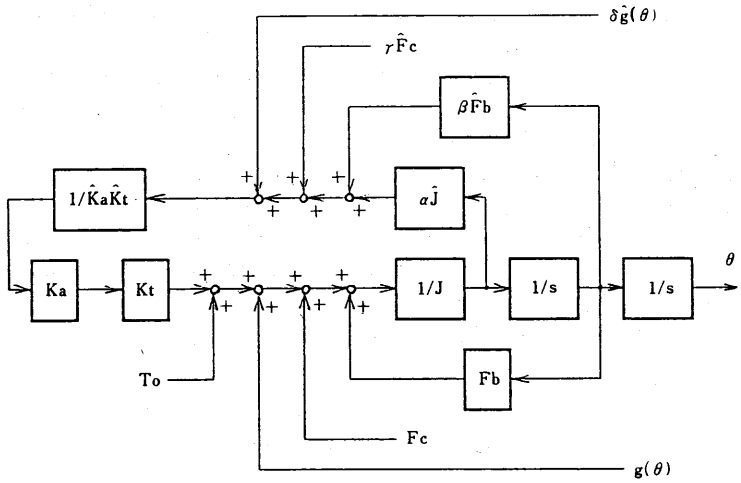

Figure 5. Block diagram of the active power assistance system (3).

merely released. In other words, it is possible to redesign the motion equations of the system into an arbitrary form through feedback.

In the case of a multiple-link manipulator, each term is not a constant but a function of the joint angle $\boldsymbol{\theta}$ ($\hat{J}_{ij}(\boldsymbol{\theta})$, $\hat{D}_{ijk}(\boldsymbol{\theta})$, and $\hat{g}_i(\boldsymbol{\theta})$ in equation (6)). The desired characteristic of each term as a result of power assistance is also expressed as a function of $\boldsymbol{\theta}$ ($J'_{ij}(\boldsymbol{\theta})$, $D'_{ijk}(\boldsymbol{\theta})$, and $g'_i(\boldsymbol{\theta})$). Thus, the difference between the desired characteristic and the original characteristic is generated by the motors.

An expression equivalent to equation (16) will be

$$T_{mi}(I_i)=\sum_{j=1}^{n}(\hat{J}_{ij}(\boldsymbol{\theta})-J'_{ij}(\boldsymbol{\theta}))\ddot{\theta}_j+\sum_{j=1}^{n}\sum_{k=1}^{n}(\hat{D}_{ijk}(\boldsymbol{\theta})-D'_{ijk}(\boldsymbol{\theta}))\dot{\theta}_j\dot{\theta}_k$$
$$+(\hat{g}_i(\boldsymbol{\theta})-g'_i(\boldsymbol{\theta}))+\beta_i\hat{F}_{bi}\dot{\theta}_i+\gamma_i\hat{F}_{ci}. \tag{18}$$

In this case, an effect appears as if each joint had an effective inertia $J'_{ijk}(\boldsymbol{\theta})$, a coupled torque coefficient $D'_{ijk}(\boldsymbol{\theta})$, a gravitational torque $g'_i(\boldsymbol{\theta})$, a viscous friction coefficient $(1-\beta_i)F_{bi}$, and Coulomb friction $(1-\gamma_i)F_{ci}$.

The way to determine $J'_{ij}(\boldsymbol{\theta})$, $D'_{ijk}(\boldsymbol{\theta})$, and $g'_i(\boldsymbol{\theta})$ will be described below. $\hat{J}_{ij}(\boldsymbol{\theta})$, $\hat{D}_{ijk}(\boldsymbol{\theta})$, and $\hat{g}_i(\boldsymbol{\theta})$ are obtained from the dynamic equation

$$\hat{J}_{ij}(\boldsymbol{\theta})\ddot{\theta}_j+\hat{D}_{ijk}(\boldsymbol{\theta})\dot{\theta}_j\dot{\theta}_k+\hat{g}_i(\boldsymbol{\theta})=\frac{\mathrm{d}}{\mathrm{d}t}\frac{\partial L}{\partial\dot{\theta}_i}-\frac{\partial L}{\partial\theta_i}. \tag{19}$$

L is the manipulator's Lagrangian. Likewise, we assume a virtual manipulator with the same shape and dimensions as those of the actual manipulator, differing in link mass only. On the basis of the Lagrangian L of the virtual manipulator, we can obtain $J'_{ij}(\boldsymbol{\theta})$, $D'_{ijk}(\boldsymbol{\theta})$, and $g'_i(\boldsymbol{\theta})$ from

$$J'_{ij}(\boldsymbol{\theta})\ddot{\theta}_j+D'_{ijk}(\boldsymbol{\theta})\dot{\theta}_j\dot{\theta}_k+g'_i(\boldsymbol{\theta})=\frac{\mathrm{d}}{\mathrm{d}t}\frac{\partial L'}{\partial\dot{\theta}_i}-\frac{\partial L'}{\partial\theta_i}. \tag{20}$$

When these are applied to equation (18), a characteristic apparently identical to that of the virtual manipulator is obtained. Link l ($l=1$ to n) has mass M_l for the original

manipulator and mass M_l' for the virtual one. When M_l contained in $\hat{J}_{ij}(\theta)$, $\hat{D}_{ijk}(\theta)$, and $\hat{g}_i(\theta)$ is replaced by M_l', the functions are equivalent to $J'_{ij}(\theta)$, $D'_{ijk}(\theta)$, and $g'_i(\theta)$. Generally, M_l is contained as a linear coefficient in $\hat{J}_{ij}(\theta)$, $\hat{D}'_{ijk}(\theta)$, and $\hat{g}_i(\theta)$. Therefore, each of the $\hat{J}_{ij}(\theta)-J'_{ij}(\theta)$, $\hat{D}_{ijk}(\theta)-D'_{ijk}(\theta)$, and $\hat{g}_i(\theta)-g'_i(\theta)$ terms are obtained as $\hat{J}_{ij}(\theta)$, $\hat{D}_{ijk}(\theta)$, and $\hat{g}_i(\theta)$, whose M_l is replaced by M_l-M_l'.

With different M_l' selecting methods used for $J'_{ij}(\theta)$, $D'_{ijk}(\theta)$, and $g'_i(\theta)$, respectively, assume that $(M_l-M_l')/M_l=\alpha_l$ for $J'_{ij}(\theta)$ and $(M_l-M_l')/M_l=\delta_l$ for $g'_i(\theta)$. Then the method of selection in the case of a single-link manipulator will be applicable. The influence of the coupled torque term is generally practically negligible under the conditions of a relatively slow velocity in the manual handling discussed here. In some cases, their compensation can be omitted.

4. EXPERIMENTS

4.1. Experimental arrangement and outline of experiments

To show the effectiveness of active power assistance using real hardware, experiments with a manipulator with one degree of freedom (d.o.f.) were conducted. Figure 6 shows the experimental system.

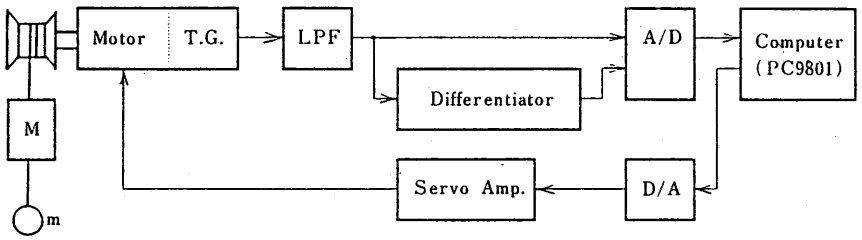

Figure 6. Experimental system.

The angular velocity signal from the tacho-generator and the angular acceleration signal from the analogue differentiator, in which the angular velocity signal is provided, were sampled by a computer (PC9801F) through A/D converters. A low-pass filter (secondary Butterworth filter, 10 Hz) was used to eliminate ripple noise. Power assistance was calculated in the computer to output a control signal to a current control servo amplifier through a D/A converter. The C language was used for the calculation. The sampling interval was approximately 0.26 ms.

To examine the effectiveness, a direct-drive type winch ($r=1.0\times10^{-2}$ m) was employed as shown in Fig. 6. Table 1 gives the specifications of the motor. Rising and falling correspond to the manipulator's degree of freedom while the main weight ($M=1.0$ kg) is equivalent to the mass of the arm. The gravity and inertial force, both applied to the main weight, and the motor's friction are compensated by the motor's hoisting force to carry out the power assistance. The moment of inertia arising from the main weight is equivalent to $J=Mr^2$. This system provides a manipulator with an equivalently very short arm. As a result, the moment of inertia is less influential than that in an ordinary arm configuration. However, in the sense that the system has low friction and is free from backlash and elasticity, it has the satisfactory characteristics of a direct-drive manipulator. Since the gravitational torque $g(\theta)$ is fixed, it is possible to compensate the gravity by adding an offset to the servo amplifier input.

Table 1.
Specifications of the direct-drive motor

Motor diameter	8.08×10^{-2} m
Motor weight	0.34 kg
Peak torque, T_p	1.11 Nm
Peak current, I_p	9.8 A
Torque sensitivity, K_t	0.113 Nm/A

As a power assistance method, equation (16) was applied. In this case, the motion equation may be approximated by

$$T_o=(1-\alpha)J\ddot{\theta}+(1-\beta)F_b\dot{\theta}+(1-\gamma)F_c+(1-\delta)g(\theta). \tag{21}$$

The closer α, β, γ, and δ become to 1, the more effective is the power assistance.

The design problem lies in how to determine these values. From equation (21), we may obtain

$$\dot{\theta}=\frac{T_o-(1-\gamma)F_c-(1-\delta)g(\theta)}{(1-\alpha)Js+(1-\beta)F_b}. \tag{22}$$

Since the term containing γ and δ acts additionally on the manual force T_o, no problem will arise if $\gamma=\delta=1$ is assumed. Since α and β are contained in the denominator, $\dot{\theta}$ may be unstable and oscillation may take place if $\alpha=\beta=1$. It is necessary, therefore, to select appropriate values for α and β within the range $0<\alpha, \beta<1$.

Through the three experiments described below, the effectiveness of power assistance was examined. We show how to select values of α and β as design parameters.

(1) Response to step manual force.
(2) Velocity attenuation without manual force.
(3) Actual manual handling.

4.2. Response to step manual force

An auxiliary weight ($m=0.1$ kg) is added to the main weight. The gravity acting on it is regarded as the manual force. It pulls down the main weight from the stationary condition. A tacho-generator is used to measure the rotation of the motor. Since the main weight has a very small acceleration compared to the gravitational acceleration, the auxiliary weight provides almost a constant manual force. From the velocity response of the main weight with the step manual force, it is possible to know the effectiveness of power assistance, which appears at the moment that the manual force is applied.

If $\dot{\theta}=0$ at time $t=0$, we may solve equation (21) as follows:

$$\dot{\theta}=\frac{T_o-(1-\gamma)F_c-(1-\delta)g(\theta)}{(1-\beta)F_b}\left(1-e^{-\frac{(1-\beta)F_b}{(1-\alpha)J}t}\right). \tag{23}$$

Figure 7 is a plot of the results of the velocity response test. The fine line represents the theoretical response curve based on equation (23).

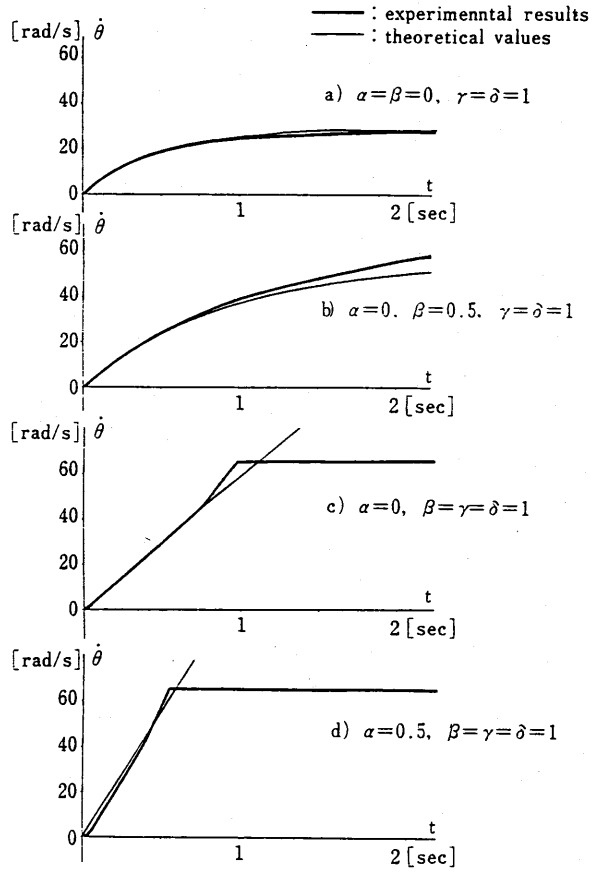

Figure 7. Effect of the active power assistance (step response). (a) Gravity/Coulomb friction compensation ($\alpha=\beta=0$, $\gamma=\delta=1$). (b) Gravity/Coulomb friction/viscous friction compensation ($\alpha=0$, $\beta=0.5$, $\gamma=\delta=1$). (c) Gravity/Coulomb friction/viscous friction compensation ($\alpha=0$, $\beta=\gamma=\delta=1$). (d) Gravity/Coulomb friction/viscous friction/inertia compensation ($\alpha=0.5$, $\beta=\gamma=\delta=1$).

As the basis for studying the effectiveness of power assistance, we discuss the following two points:

(1) the angular velocity increasing rate $\ddot{\theta}_{t=0}$ at the moment when the step manual force is applied; and
(2) the angular velocity convergent value $\dot{\theta}_{t\to\infty}$ with a constant manual force.

From equation (23), we obtain

$$\ddot{\theta}_{t=0}=\{T_o-(1-\gamma)F_c-(1-\delta)g(\theta)\}/\{(1-\alpha)J\} \tag{24}$$

$$\dot{\theta}_{t\to\infty}=\{T_o-(1-\gamma)F_c-(1-\delta)g(\theta)\}/\{(1-\beta)F_b\}. \tag{25}$$

When only gravity is compensated ($\alpha=\beta=\gamma=0$, $\delta=1$), the auxiliary weight is balanced by the Coulomb friction while both the angular velocity increasing rate and the angular velocity convergent value become nearly zero. In Fig. 7(a) ($\alpha=\beta=0$, $\gamma=\delta$

$=1$), where the Coulomb friction is compensated, the angular velocity increasing rate and the angular velocity convergent value are improved to 61 rad/s^2 and 28 rad/s, respectively. As shown in Fig. 7(a), the actual response coincides well with the theoretical response.

In the case of Fig. 7(b) ($\alpha=0$, $\beta=0.5$, $\gamma=\delta=1$), where the viscous friction is compensated, the angular velocity increasing rate does not change theoretically while the angular velocity convergent value is doubled (from equations (24) and (25)). The actual angular velocity increasing rate is 61 rad/s^2 and the angular velocity convergent value is 58 rad/s. Both resemble the results mentioned above and their response curves coincide well with the theoretical ones. In the case of Fig. 7(c) ($\alpha=0$, $\beta=\gamma=\delta=1$), where the viscous friction is completely compensated, the angular velocity does not converge to a fixed value but continues to increase at a constant angular acceleration. The A/D converter is saturated by the tacho-generator output at 66 rad/s. The response up to this point shows a nearly linear increase. The angular acceleration is 58 rad/s^2, which hardly changes as expected from equation (24).

In Fig. 7(d) ($\alpha=0.5$, $\beta=\gamma=\delta=1$), where the inertia is also compensated, the angular velocity increasing rate is doubled, as expected from equation (24). The actual angular velocity increasing rate is 107 rad/s^2, which is nearly equal to the theoretical value.

4.3. Effectiveness of the inertia compensation

The velocity attenuation characteristic at zero manual force (without the auxiliary weight) is examined. The main weight is controlled so as to fall at a constant initial velocity (60 rad/s) at first. Then the power assistance begins to work. From the subsequent velocity attenuation characteristic, it is possible to study the effectiveness of power assistance in suppressing the inertia after the manual force is stopped. When $\theta=\omega_0$ at $t=0$, we may solve equation (21) as follows:

$$\dot{\theta}=\omega_0+\left(\omega_0+\frac{(1-\gamma)F_c+(1-\delta)g(\theta)}{(1-\beta)F_b}\right)\left(e^{-\frac{(1-\beta)F_b}{(1-\alpha)J}t}-1\right) \tag{26}$$

(where $\dot{\theta}>0$). Figure 8 shows the resulting velocity response. The fine line represents the theoretical response based on equation (26).

Figure 8(a) shows the response with gravity and Coulomb friction compensated ($\alpha=\beta=0$, $\gamma=\delta=1$). Figure 8(b) shows the response with viscous friction also compensated. The angular velocity attenuation rate is lower in Fig. 8(b) than in Fig. 8(a). This means that the arm continues to move even after the force stops acting on the arm. At large inertia it may be difficult to control the arm due to an overshoot.

In Fig. 8(c) ($\alpha=\beta=0.5$, $\gamma=\delta=1$), where the inertia is compensated, angular velocity attenuation is obtained at a level equivalent to that in Fig. 8(a), as expected from equation (26). It is confirmed that the reversing force required upon deceleration becomes smaller when the inertia is compensated.

4.4. Stability and limits of the α and β values

As already mentioned, the power assistance based on equation (16) becomes more effective as α, β, γ, and δ approach 1. γ and δ may be taken as $\gamma=\delta=1$; this was confirmed by the experiments described in Sections 4.2 and 4.3. Here, we discuss to what extent α and β approach 1.

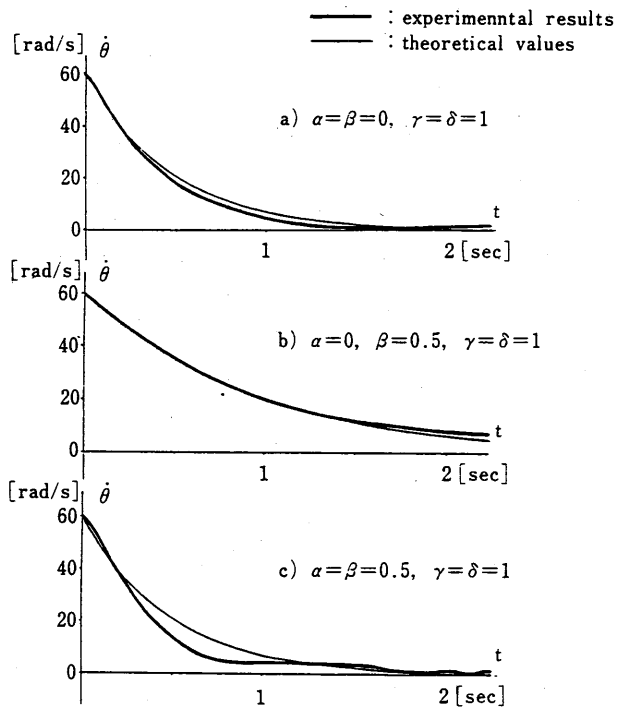

Figure 8. Effect of the active power assistance (damping characteristic). (a) Gravity/Coulomb friction compensation ($\alpha=\beta=0$, $\gamma=\delta=1$). (b) Gravity/Coulomb friction/viscous friction compensation ($\alpha=0$, $\beta=0.5$, $\gamma=\delta=1$). (c) Gravity/Coulomb friction/viscous friction/inertia compensation ($\alpha=\beta=0.5$, $\gamma=\delta=1$).

Both experiments described in Sections 4.2 and 4.3 proved that an overshoot takes place in the velocity response as the inertia compensating parameter α increases (Figs 9(a) and 9(b)). Finally oscillation occurs as α becomes still closer to 1 (Figs 9(c) and 9(d)). This oscillation could not be avoided regardless of the value of β. The limit value at which the oscillation takes place is $\alpha=0.9$–0.95 and the oscillating frequency is 0.7–1.3 Hz. The reasons why such oscillation takes place at $\alpha \doteqdot 1$ are considered. First of all, the system is unstable because the coefficient of the integral term in equation (22) is closer to 0. Second, non-linearity is caused by saturation in the servo amplifier or the analogue circuit, and a phase dislocation due to the low pass filter is contained in the angular acceleration signal to compensate for the inertia. It seems to be possible to choose α still closer to 1 by improving the method of measuring the angular velocity signal and the linearity of a motor control system. Since a very large acceleration would possibly be required with $\alpha \doteqdot 1$, it would be necessary to set α to the extent that any excessive force may not work on the motor and other mechanisms.

As for the viscous friction compensating parameter β, it has already been confirmed in the experiment described in Section 4.2 that the angular velocity shows a stable increase even with $\beta=1$. The experiment referred to in Section 4.3 revealed that the angular velocity does not attenuate with $\beta=1$, while the main weight continues to fall at the initial speed. The angular velocity does not oscillate and remains constant. Even when α is changed within the range ~ 0 to 0.8, the same result is obtained. As

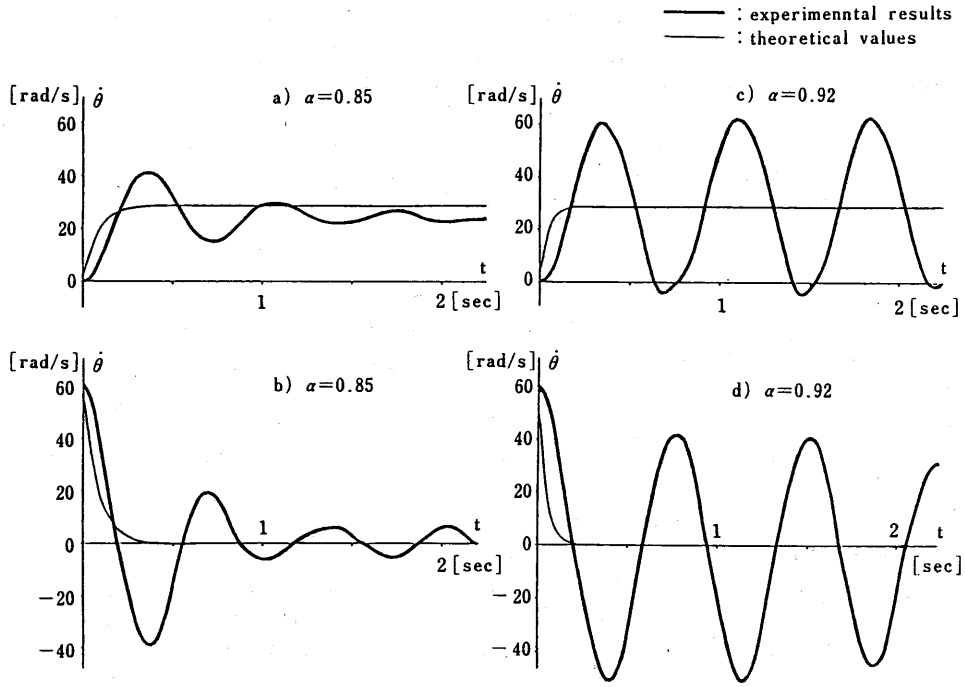

Figure 9. Overshoot and hunting with excessive inertia compensation. (a) Step response ($\alpha=0.85$). (b) Damping characteristic ($\alpha=0.85$). (c) Step response ($\alpha=0.92$). (d) Damping characteristic ($\alpha=0.92$). $\beta=0$; $\gamma=\delta=1$.

presented above, it is actually possible to set $\beta=1$. If the attenuation term is eliminated, the arm does not stop by itself when released. Therefore it is necessary to take measures to meet it in real applications. Nevertheless, no oscillation is caused by the fact that the arm does not stop.

4.5. Actual manual handling

Quantitative experiments as described above were carried out to determine the effectiveness of active power assistance. In addition, we also examined handling feeling with power assistance by holding the main weight and moving it up and down. As compared with the case where only gravity is compensated, both acceleration/deceleration and regular velocity operations were found to be possible with a smaller force if the compensation covered all the terms of inertia, viscous friction, Coulomb friction, and gravity.

An investigation into the handling feeling while changing the values of α and β variously, with $\gamma=\delta=1$, also proved that the handling is lighter when both α and β are close to 1. As for the inertia compensating parameter α, stable handling was possible up to $\alpha=0.85$. Even with $\alpha=0.9$, the handling remained stable as long as the main weight was being moved. When the operator tried to stop the main weight, overshooting and oscillation took place, making the handling difficult. Although a very large overshoot was observed with $\alpha=0.85$ in the experiment described in Section 4.4, it was not felt so

much in the manual handling. This is because the value of α actually becomes smaller as the mass of the operator's hand is added to the mass of the main weight. Besides, the manual handling is not pure force control to apply a constant force in one direction but possibly includes position control while adjusting the force.

Even with the viscous friction compensating parameter $\beta = 1$, light handling was possible without arousing any problem. If positioning is performed, however, the main weight can be easily stopped, with $\beta = 0.8$ while leaving an attenuation term.

5. SUMMARY

This paper has presented a method of detecting manual force and of providing active power assistance in a direct-drive manipulator without any special sensor, using only internal sensors such as a tacho-generator. The effectiveness of the proposed power assistance was proved through experiments on a 1 d.o.f. manipulator.

Through these experiments, we obtained the following results:

(1) It is possible to eliminate the inertia terms to approximately 85% through compensation.
(2) It is possible to compensate for 100% of the viscous friction. If positioning is performed, however, it will be easier to use approximately 80% for compensation.
(3) Both Coulomb friction and gravity can be compensated to 100%.

Thus, we could obtain data which provide us with the guidelines for designing a system of this type.

The problems to be solved in the future are as follows:

(1) higher resolution and more precise angle detecting devices;
(2) reliable identification of such parameters as friction, etc.; and
(3) balance of each axis in power assistance in a multiple-link manipulator.

The results obtained through the present study signify that the characteristics of a system physically described in a certain motion equation can be redesigned by feedback into another system that apparently has arbitrary characteristics. In addition, they can be applied to a wide range.

Acknowledgements

The authors would like to thank Mr. Minoru Abe, Director General, Robotics Department, Mechanical Engineering Laboratory; Mr. Akio Fujikawa, former Director, Cybernetics Division (currently International Robot & F.A. Engineering Center); and other staff of the Cybernetics Division and Man–Machine Systems Division for their cooperation.

REFERENCES

1. H. Hirai, K. Honma and M. Imai, "Development of power assist type handling mechanism," in *Proc. 22th Soc. Instrum. Control Eng. Annu. Conf.*, pp. 547–548, 1983 (in Japanese).
2. H. Inoue, "Computer control of an artificial hand," *J. Jpn Soc. Mech. Eng.*, vol. 73, no. 718, pp. 946–954, 1970 (in Japanese).

3. S. Kurono, "Coordination control of a couple of artificial hands," *J. Jpn Soc. Mech. Eng.*, vol. 78, no. 682, pp. 804–810, 1975 (in Japanese).
4. M. Uchiyama, "Study on dynamic control of an artificial hand (coordination motion control with a mathematical model)," *Trans. Jpn Soc. Mech. Eng.*, vol. 45, no. 391, pp. 323–335, 1979 (in Japanese).
5. H. Asada, "Development of a Direct-drive robot and evaluation of its control performance," *Trans. Soc. Instrum. Control Eng.*, vol. 19, no. 1, pp. 77–84, 1983 (in Japanese).
6. T. Suehiro and K. Takase, "A manipulation system based on direct computational task-coordinate servoing," *J. Robotics Soc. Jpn*, vol. 3, no. 2, pp. 95–105, 1985 (in Japanese).
7. H. Kuwahara, T. Matenmoto, Y. Ono, M. Nikaido and K. Fujita, "Articulated direct-drive robot with 6 d.o.f.," in *Proc. 2nd Annu. Conf. Robotics Soc. Jpn*, pp. 21–22, 1984 (in Japanese).
8. E. Tsuda and M. Takeshita, "Application of AC servo motors for a direct drive manipulator," *Mech. Eng.*, vol. 28, no. 7, pp. 56–60, 1984 (in Japanese).
9. Y. Ono, H. Kuwahara and M. Nikaido, "High resolution rotory encoder for a direct drive robot," in *Proc. 23th Soc. Instrum. Control Eng. Annu. Conf.*, pp. 557–558, 1984 (in Japanese).
10. M. Fujita and H. Inoue, "Study on processing of force sensor signal," in *Proc. 1st Annu. Conf. Robotics Soc. Jpn*, pp. 151–152, 1983 (in Japanese).
11. M. Uchiyama, K. Hakomori and M. Yohota, "Dynamic sensing of 6-axis robot wrist force," *Proc. 2nd Annu. Conf. Robotics Soc. Jpn*, pp. 137–138, 1984 (in Japanese).

ABOUT THE AUTHORS

Hirohiko Arai (M'83) was born on 9 July 1959 in Tokyo, Japan. He graduated from the University of Tokyo in 1982, majoring in instrument engineering. In 1982, he joined Honda Engineering Corporation. In 1984, he joined the Mechanical Engineering Laboratory, Ministry of International Trade and Industry, Tsukuba Science City, and is currently a researcher for the Man–Machine Systems Division of the Robotics Department. His interests include manipulator control, man–machine systems, and tele-operation. He is a member of the Society of Instrument and Control Engineers.

Susumu Tachi (M'83) was born on 1 January 1946 in Tokyo, Japan. He received B.E., M.S., and Ph.D. degrees in mathematical engineering and instrumentation physics from the University of Tokyo in 1968, 1970, and 1973, respectively. He joined the Faculty of Engineering, University of Tokyo, in 1973. From 1973 to 1976, he held a Sakkokai Foundation Fellowship. In 1975, he joined the Mechanical Engineering Laboratory, Ministry of International Trade and Industry, Tsukuba Science City, and is currently Director of the Man–Machine Systems Division of the Robotics Department. From 1979 to 1980 he was a Japanese Government Award Senior Visiting Fellow at the Massachusetts Institute of Technology, Cambridge, MA, U.S.A. His present interests include human rehabilitation engineering, statistical signal analysis, and robotics, in particular, sensory control of robots, autonomous mobile robots, and tele-robotics. Dr. Tachi is a member of IEEE, the Japan Society of Medical Electronics and Biomedical Engineering, the Society of Instrument and Control Engineers, the Japan Society of Mechanical Engineers, the Society of Mechanical Engineers, and the Society of Biomechanisms.